



# Ultrathin flexible pressure sensors using microbead embedded nanofibrous membrane for wearable applications

Taiyu Jin<sup>a</sup>, Yan Pan<sup>b</sup>, Sang-Hee Ko Park<sup>c</sup>, Da-Wei Fang<sup>a,\*</sup>

<sup>a</sup> Institute of Rare and Scattered Elements, College of Chemistry, Liaoning University, Shenyang 110036, PR China

<sup>b</sup> Shenzhen Institute of Advanced Electronic Materials, Shenzhen Institute of Advanced Technology, Chinese Academy of Sciences, Shenzhen 518055, PR China

<sup>c</sup> Department of Materials Science and Engineering, Korea Advanced Institute of Science and Technology (KAIST), Daejeon 34141, South Korea

## ARTICLE INFO

### Keywords:

Pressure sensor  
Nanofiber  
Microbead  
Electrospinning  
Wearable device  
Health monitoring

## ABSTRACT

With the increasing demand for real-time health monitoring driven by the popularity of wearable devices, there is a growing need for thin, flexible pressure sensors. In this study, we propose a strategy for developing a flexible ultrathin piezoresistive pressure sensor utilizing a composite of nanofibers and microbeads. The investigation primarily focuses on the effect of incorporating microbeads on nanofiber morphology and the correlation between the surface roughness of the nanofiber membrane and the performance of the pressure sensor. It has been elucidated that the integration of microbeads into nanofiber membranes enhances the performance of the pressure sensor. The prepared sensor has a sensitivity of  $1.12 \text{ kPa}^{-1}$ , high stability that does not degrade after being pressed for more than 1000 times, and short response time (response/recovery times are 210 ms/140 ms, respectively) that is enough to detect human pulse. Furthermore, we have elaborated on how the choice of materials for the conductive layer, the coating technique, and the spraying duration impact the performance of the piezoresistive pressure sensor. Finally, we demonstrated that the ultrathin flexible pressure sensor can effectively operate on curved surfaces and has been successfully tested on human wrist pulses and carotid pulses. The successful fabrication of this sensor not only expands the fabrication techniques for pressure sensors but also enhances the performance of lightweight and thin pressure sensors, laying a technical foundation for developing pressure sensors suitable for portable devices.

## 1. Introduction

With the advancement of smart electronics and information technology, wearable devices have attracted a lot of attention due to their portability and real-time detection capability [1–4]. The accurate detection ability of wearable devices is mainly attributed to the high-performance sensors inside. Among these sensors, pressure sensor is the most basic sensor, so it has been studied intensively [5]. However, due to the limitations of material and technology, pressure sensors currently available for commercial use usually show the disadvantages of large size, heavy weight, and non-bendability, which do not conform to the development trend of being thin and light. Therefore, it has become an urgent need to develop a high-performance flexible pressure sensor that can avoid these shortcomings [6–10].

Pressure sensor is a device that can convert mechanical signals into electrical signals. Usually, it can be categorized into piezoresistive [11], capacitive [12,13], piezoelectric [14], and other types [15–17]

according to the transduction mechanism. As one of the most common pressure sensors, piezoresistive pressure sensors can convert mechanical pressures into resistance signals [18]. Given its appealing advantages such as a straightforward structure, facile signal acquisition, good repeatability, and low cost, the piezoresistive pressure sensor emerges as a promising candidate for diverse applications, boasting significant potential [19–21]. Skin-conformable devices have attracted considerable research attention due to their ease of use and potential for seamless integration with the human body. To achieve effective operation and minimize the sensation of discomfort or foreign body perception, such devices typically require an ultrathin design. It is generally recognized that a thickness below  $100 \mu\text{m}$  is essential for ensuring optimal skin conformity. Accordingly, the development of an ultrathin pressure sensor with excellent skin-conformable properties is of significant importance and holds great promise.

Many piezoresistive pressure sensors are realized through the creation of a three-dimensional conductive network or the design of a

\* Corresponding author.

E-mail address: [dwfang@lnu.edu.cn](mailto:dwfang@lnu.edu.cn) (D.-W. Fang).

<https://doi.org/10.1016/j.jalcom.2025.178609>

Received 11 September 2024; Received in revised form 5 December 2024; Accepted 9 January 2025

Available online 10 January 2025

0925-8388/© 2025 Elsevier B.V. All rights reserved, including those for text and data mining, AI training, and similar technologies.

contact interface with variable resistance [22]. In order to obtain a conductive network, the usual method is to embed conductive fillers into porous elastic materials. Yang et al. reported a novel flexible pressure sensor with a tunable and large detection range by introducing magnetic carboxyl iron particle/silicone resin into a carbon sponge [23]. Yu et al. obtained a flexible piezoresistive sensor with good performance in both compressed and stretched states by embedding carbon nanotubes (CNTs) on the surface of a 3D printed TPE network [24].

However, because a three-dimensional conductive network inevitably takes up a certain amount of space, it is difficult to manufacture an ultra-thin sensor using this method. This problem can be solved by forming a conductive layer with variable resistance on the contact electrode of the sensor [25–28]. Researchers have developed a variety of micro-protrusions to roughen the surface of pressure-sensitive materials. Lu et al. prepared ultrathin nanocone array films by adjusting the structure of anodic alumina templates and fabricated highly-sensitive pressure sensors by interlocking the nanocone arrays [29]. Chen et al. proposed a new strategy to fabricate MXene@PDMS piezoresistive pressure sensor with a micro-protrusion structure using a sandpaper template [30]. Nevertheless, when using the surface roughening methods described above, it is necessary to prepare a template first and form micro-protrusions based on this template [31]. Therefore, the fabrication processes are usually complex, costly, and time-consuming. In addition, since the size of these protrusions is normally very small, the deformation caused by external forces can easily reach saturation and eventually affect the detection range of the pressure sensor. We have summarized the previously reported piezoresistive pressure sensors and summarized their performance in Table 1.

Over the past few decades, nanofiber membranes have been widely used in a variety of applications due to their flexibility, inherent biocompatibility, and low cost [36]. It is reported that nanofiber membranes can be used as advanced separators for lithium-ion batteries [37] as well as air filters for high-efficiency PM2.5 capture [38,39]. In addition, nanofibers have also been reported to be used in flexible pressure sensors, not only for pressure-sensitive materials [40] but also for substrate materials [41]. Liu et al. inserted a layer of polyvinyl alcohol (PVA) nanofibers between a sheet of wrinkled graphene film and a pair of interdigital electrodes (IDE) as a dielectric layer to achieve excellent durability and reliability [42]. Hu et al. developed a highly sensitive pressure sensor based on a polyimide (PI) substrate and P(VDF-TrFE)/BTO nanofiber mat. The sensitivity of the sensor is greatly improved by the difference in elastic modulus between the nanofiber mat and the microstructured PI substrate [43]. Ren et al. obtained a wearable and high-performance capacitive pressure sensor based on a biocompatible PVP nanofiber membrane [44]. However, since the diameter of a single nanofiber is on the order of nanometers, it usually takes several hours to fabricate the nanofibers into a mat material in previous reports [45]. Therefore, addressing the prolonged preparation time of nanofiber membranes holds crucial practical significance for advancing the application of nanofiber materials. In our previous study, we demonstrated that incorporating micron-sized spacers into nanofibers significantly reduced the fabrication time of fiber membranes while effectively preventing micron-sized spacers from moving freely

[46]. Building on this finding, we propose that integrating micron-sized beads directly onto the membrane surface could eliminate the need for preparing micro-protrusion molds, thereby simplifying the fabrication process of piezoresistive pressure sensors.

Herein, we propose a strategy to fabricate a piezoresistive pressure sensor using a nanofiber membrane with micro-protrusions on the surface. The nanofibers were prepared by using electrospinning technology, and in order to form micro-protrusions on the surface of the nanofiber membrane, microbeads were mixed in the electrospinning solution. Eventually, we obtained a microbead-nanofiber composite in one step. Compared with pure nanofibers, microbeads containing composite not only have a shorter preparation time but also can make the resulting sensor thin and light. In order to make the nanofiber membrane conductive without affecting the surface morphology, we evaluated various conductive films. Finally, a spraying method using silver nanowires was selected and an optimal preparation condition was given. The proposed piezoresistive pressure sensor can be obtained by combining this surface-conductive nanofiber membrane with a flexible electrode. In addition, the topography of the conductive layer, the thickness of the nanofiber film, and the elastic modulus can all affect the sensitivity and linearity of the sensor. Then, we fabricated a flexible pressure sensor with high sensitivity and wide linearity. The sensor shows a low detection limit, fast response time, and good stability. Moreover, its outstanding flexibility enables it to perform pressure detection on curved surfaces. In the end, the frequency and waveform of the human pulse were accurately measured in real-time. This study is an important step towards the realization of lightweight and flexible wearable electronic devices.

## 2. Experimental section

### 2.1. Fabrication of PVDF film

PVDF powder (Solvay) was dissolved in a MEK/Acetone mixture (1:1 v:v) under magnetic stirring for 24 h to form the homogeneous PVDF solution. Then, the prepared 20 wt% PVDF solution was cast into a thin film using the bar coating method. The film was then placed on a hot plate and heated to 160 °C to remove internal stress and flatten the surface.

### 2.2. Electrospinning process

PVDF powder was dissolved into a calculated volume of DMAc and stirred vigorously to obtain 20 wt% PVDF solution. PMMA microbeads with a diameter of 20 μm (S20; Duksan Hi-Metal Co., Ltd.) were introduced into the PVDF solution to prepare a nanofiber solution. To disperse the suspension homogeneously, the solution was stirred vigorously for two days. Then the solution was added into the syringe of an electrospinning instrument and spun onto the collector at a flow rate of 50 μL/min. Working distance was kept at 10 cm and a high voltage of 10 kV was applied between the nozzle and the collector. A nanofibrous membrane can be obtained on a PVDF film by pre-positioning the PVDF membrane on an electrospinning collector.

### 2.3. Device fabrication

The specific preparation steps of the device are as follows. After the surface of the nanofiber membrane was treated with O<sub>2</sub> plasma, AgNWs (1 wt%, Nanopyxis Co., Ltd.) were coated thereon to form an electrode. The electrode was shaped using a screening mask to form a square with sides of 1 cm in length. A small tail was formed at the bottom of the electrode for connecting test leads. The upper and lower electrodes were assembled with an overlap area of 1 cm × 1 cm to form a piezoresistive pressure sensor.

**Table 1**

Comparison of specific parameters between this study and previously reported piezoresistive sensors.

| Materials   | Sensitivity (kpa <sup>-1</sup> ) | Response time (ms) | Limit of detection (kPa) | Ref.      |
|---|----------------------------------|--------------------|--------------------------|-----------|
| ZnO/Ti <sub>3</sub> C <sub>2</sub> T <sub>x</sub> | 6.40                             | 190                | -                        | [32]      |
| EVOH/MWCNT  | 0.28                             | 400                | 0.08                     | [33]      |
| CB/MXene/SR/fiber                                 | 2.18                             | 100                | 0.1                      | [34]      |
| Cu/rGO  | 0.144                            | 150                | 0.1                      | [35]      |
| AgNWs/NF/Microbead                                | 1.12                             | 210                | 0.05                     | This work |

## 2.4. Characterization

The surface morphology of the PVDF nanofibers containing microbeads was characterized using an SEM (Philips XL 30 FEG). Pressure sensors were tested using a hand-made system. The pressure application system consists of a motorized test stand (Mark-10, ESM 303) and a digital force gauge (Mark-10, M5-2) with a plastic tip. The size of the contact tip is about  $6\text{ mm} \times 6\text{ mm}$ . The resistance value was measured and recorded in real-time using a Desktop Digital Multimeter (Keysight, 34461 A). A PC was used to record sensor output and force values simultaneously.

## 3. Results and discussion

### 3.1. Device structure

The fabrication method of the flexible piezoresistive pressure sensor is illustrated in Fig. 1. The pressure sensor consists of two parts: upper and lower electrodes. The upper electrode is obtained by coating a conductive layer on a nanofiber film with uneven surface morphology, which mainly provides variable resistance for the device when it is subjected to external force. Nanofibers are fabricated onto flexible substrates through the utilization of electrospinning equipment. Subsequently, conductive films are formed by applying a layer of conductive material onto the surface of the nanofibrous membrane. The lower electrode is obtained by coating a square-shaped conductive AgNWs layer on a PVDF carrier film, with a square size of  $1\text{ cm} \times 1\text{ cm}$ . The function of the lower electrode is to support and provide a counter electrode for the upper electrode. The device we proposed has an overall thickness of less than  $100\text{ }\mu\text{m}$ , which shows that it not only has excellent flexibility but also has practical application potential.

Choosing the appropriate substrate material is the basis for realizing ultra-thin flexible pressure sensors. Traditionally, silicon has been the preferred substrate material for commercial pressure sensors due to its outstanding electrical and mechanical properties. However, its lack of flexibility renders it unsuitable for use in flexible devices. PVDF has been widely used as substrate materials in various flexible applications in recent years due to its flexibility, durability, chemical resistance,

thermal stability, UV resistance, low permeability, and other advantages. In addition, because PVDF is relatively easy to process and can be formed into thin films or sheets using various manufacturing techniques, it allows for the easy reduction of substrate thickness and proves cost-effective for mass production of flexible substrates. Hence, we utilize PVDF film as the substrate material for the flexible pressure sensor. Consequently, the negative impact of the substrate on the flexibility of the nanofibers can be greatly eliminated.

The selection of nanofiber as the pressure-sensitive layer primarily stemmed from its exceptional mechanical properties, straightforward preparation process, and cost-effectiveness. Nonetheless, the conventional method of nanofiber utilization involves fabricating a pristine nanofiber mat devoid of any protruding surface structures. Therefore, our approach aims to develop a microbead-nanofiber composite membrane to mitigate these drawbacks. The selection of this composite material is primarily driven by its unique structural advantages: the incorporation of microbeads not only significantly enhances the porosity of the nanofiber membrane but also effectively reduces the fabrication time. Precise control over the quantity of microbeads enables the fine-tuning of surface roughness, catering to diverse application requirements for material surface properties. The ultimate goal of this design is to eliminate the necessity for additional template-based surface structuring, thereby making the fabrication process more efficient and controllable. This study provides an in-depth exploration of the microbead-nanofiber composite structure, offering a practical solution for the straightforward preparation of high-performance membrane materials.

### 3.2. Silver nanowires on the surface of nanofibers

Piezoresistive pressure sensors are designed with materials that exhibit changes in resistivity in response to mechanical deformation, so it is important to use conductive materials with appropriate conductivity as the pressure-sensitive layer [47,48]. Excessive conductivity in the conductive material leads to a reduction in the pressure sensor's resistance at low pressure, resulting in diminished sensitivity at medium and high pressures. Conversely, insufficient conductivity hampers the sensor's ability to effectively respond to external pressures, leading to decreased sensitivity. Moreover, different coating techniques can alter the microstructure and properties of these materials [49–51]. Hence, the selection of suitable materials and the optimization of preparation processes play a crucial role in enhancing the performance and stability of pressure sensors. In addition, the surface of the nanofiber membrane has many holes and is discontinuous, so we chose silver nanowires as the conductive material in this study. In order to uniformly coat silver nanowires on the surface of the nanofiber membrane, and maximize the resistive response of the conductive layer under pressure load, we tried two coating methods: dip coating and spray coating.

Fig. S1 shows the surface SEM images of the AgNWs coatings obtained by dip coating. It can be seen that after the nanofibrous membrane was immersed in 1 wt% AgNWs dispersion three times according to normal procedures, the protrusions in the nanofiber composite membrane were wrapped by a thick layer of AgNWs. This results in the interface between the nanofibers and microbeads becoming indistinguishable, with some protrusions even being buried and disappearing. This shows that the coating process not only affects the conductivity of the electrode but also affects the surface morphology of the film. Even if the solution is diluted to half of the original concentration (0.5 wt%) and the dipping process is reduced to only one time, the resulting AgNWs layer is still thick and exhibits very low sheet resistance. Since the piezoresistive pressure sensor primarily relies on the resistance change caused by the mechanical deformation of the conductive film for pressure recognition, insufficient surface protrusion of the conductive layer may result in inadequate resistance change during operation, thereby indicating poor sensor performance. In addition, the process of dip coating is hindered by a significant disadvantage, namely, the difficulty

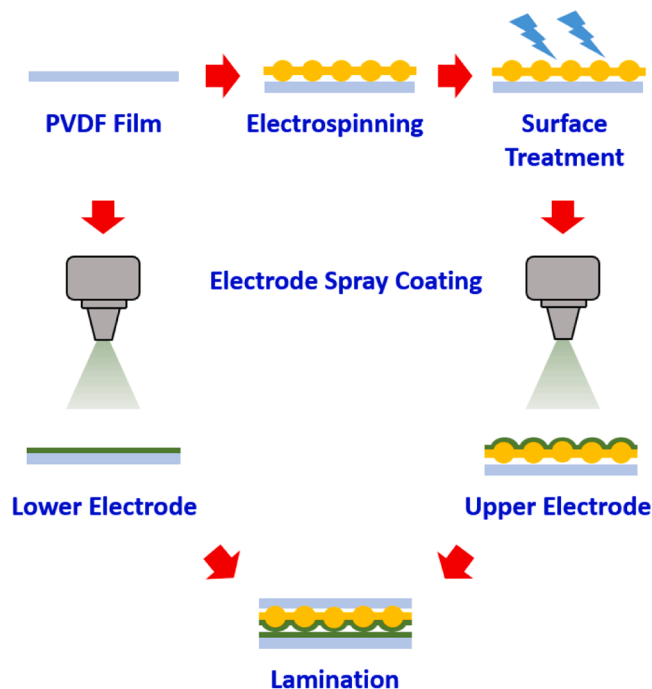


Fig. 1. Schematic diagram of the device preparation steps.

in crafting electrodes with specific shapes, which ultimately limits the adaptability of future sensors.

Fig. 2 shows the surface SEM images of AgNWs sprayed onto the surface of the nanofiber membranes. Compared to the dipping method, the spray coating method produces a thinner AgNW layer with moderate density. A square-shaped electrode with a side length of 1 cm fabricated using the spray coating method exhibited an initial resistance of approximately 30  $\Omega$ , whereas electrodes prepared by the dip coating method demonstrated initial resistances of less than 1  $\Omega$ . Given that the resistance of piezoresistive sensors decreases progressively during compression, maintaining an initial resistance within a moderate range is critical to ensure optimal sensor performance.

This is attributed to the superior controllability of the spray coating method, which effectively reduces the amount of AgNWs applied in a single spray. The resulting conductive AgNWs layer achieves moderate conductivity, preventing a reduction in the sensor's sensitivity due to excessively high conductivity. Furthermore, the surface morphology of the nanofiber composites remains unchanged after the coating treatment. This ensures that when the conductive layer contacts the counter electrode, there is sufficient space for mechanical deformation, addressing the issue of pressure level discrimination during the application of external forces. Unless otherwise specified, the spray coating method was used in this study to form the conductive AgNWs layer on the nanofiber membrane surface.

To achieve a uniform conductive thin film, we quantified the area that can be coated with 1 mL of a 1 wt% AgNW dispersion and defined it as the spraying density. For the bottom electrode, which requires high conductivity, the spraying density was set at 36  $\text{cm}^2/\text{mL}$ . In contrast, for the top electrode, which demands moderate conductivity, the density was set at 4410  $\text{cm}^2/\text{mL}$ . Excessive conductivity in the top electrode could hinder the sensor's ability to differentiate pressure variations, while insufficient conductivity could lead to sensor malfunction.

### 3.3. Sensitivity under different nanofiber condition

To determine the effect of nanofiber morphology on the performance

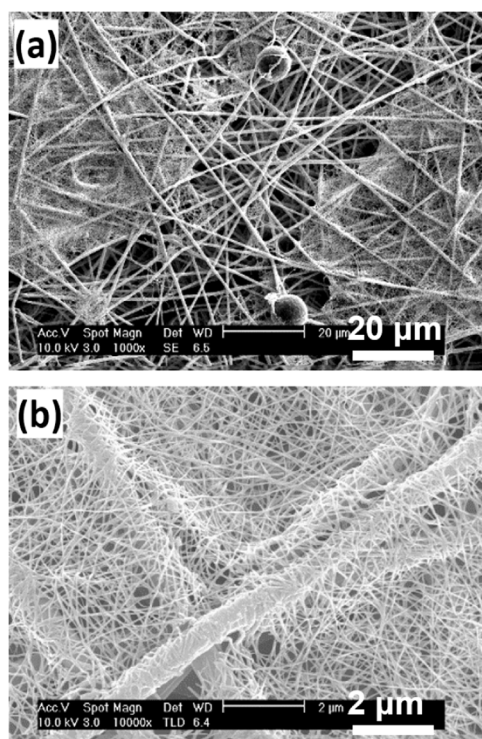


Fig. 2. SEM images of AgNWs sprayed onto the surface of nanofibers.

of pressure sensors, we used electrospinning technology to prepare nanofiber membranes both with and without microbeads, and then used these nanofiber membranes to prepare pressure sensors. The effects of pure nanofibers and microbead-containing nanofibers on sensor performance were analyzed. Due to the presence of micro-protrusions on the surface of the nanofiber composite film, the AgNWs layer sprayed on top also exhibits micro-protrusions, influenced by the surface morphology of the nanofiber composite film. When no external pressure is applied to the pressure sensor, hardly any protrusions can contact the lower electrode. The contact area between the upper and lower electrodes is relatively small and the contact resistance is relatively large. However, when external pressure is applied to the pressure sensor, the protrusions on the upper electrode are pressed into the nanofiber membrane, which flattens the surface of the conductive layer. This phenomenon engenders an enlarged contact area between the two electrodes, simultaneously resulting in a diminished contact resistance. Taking a macroscopic perspective, the resistance of the pressure sensor exhibits a decrease as the applied pressure increases. In order to conduct stable pressure testing, we built a hand-made pressure testing system (Fig. S2).

The sensor's sensitivity ( $S$ ) is defined as the derivative of the relative change in resistance ( $\Delta R = (R_0 - R)$ ) with respect to the applied pressure ( $P$ ), expressed mathematically as,

$$S = \delta(\Delta R/R_0)/\delta P$$

Where  $R$  is the real-time resistance and  $R_0$  is the initial resistance of the sensor. The sensitivity is determined by calculating the slope of the tangent line on the pressure–resistance curve. Since the resistance value of the sensor always decreases as the pressure increases in this study, we took the absolute value of  $\Delta R$  when calculating the sensitivity. Moreover,  $\Delta R$  never exceeds  $R_0$ , so the  $\Delta R/R_0$  value always remains below 100 %.

As shown in Fig. S3, although both samples of nanofiber membranes (with microbeads and without microbeads) were prepared using electrospinning for 20 min, the resistive change of the piezoresistive pressure sensor prepared with pure nanofibers (without microbeads) immediately increases and reaches saturation under low pressure. This implies that pressure sensors lacking microbeads, aside from the contact state between the upper and lower electrodes, exhibit an inability to differentiate pressure. Such characteristics mean that the device is unusable for practical applications. In contrast, the sample containing microbeads demonstrated favorable sensing properties across the measurable pressure range, even though the overall resistance change was nearly equivalent to that of the pure nanofiber sample.

As mentioned above, a common method for enhancing the sensitivity of piezoresistive pressure sensors involves the incorporation of micro-protrusion structures on the electrodes. When the surface of the pressure-sensitive material lacks these micro-protrusions, that is, the electrode surface is flat, the two electrodes can easily reach complete contact, because there is no buffer space for mechanical deformation when the upper and lower electrodes come into contact. Consequently, the lack of micro-protrusions causes rapid saturation of resistance, resulting in low linearity of the sensor. On the other hand, due to the absence of spacers for external force support, the loose nature of pure nanofiber results in easy saturation when exposed to external forces, thereby leading to compromised sensing linearity of the sensor. Nevertheless, even if the content of microbeads in the nanofiber is only 5 wt%, this nanofiber composite membrane can still provide support for external forces and enable the corresponding sensor to function effectively under mechanical deformation within a specific pressure range. Therefore, the integration of microbeads is beneficial for improving the performance of pressure sensors based on nanofibers.

In this study, microbeads play a crucial role as prominent micro-protrusions, making their size a pivotal factor. We opted for microbeads with a diameter of 10  $\mu\text{m}$ , incorporating them into nanofibers through an electrospinning process to create composite nanofibers. As illustrated in the Fig. S4, the introduction of 10  $\mu\text{m}$  microbeads slightly

enhances the performance of the sensor compared to the sensor consisting solely of nanofibers. This enhancement may stem from the relatively small size of the microbeads, which prevents them from protruding prominently on the electrode surface. However, if the microbead size is too large, it could lead to nozzle clogging during the electrospinning process. Therefore, selecting an appropriate microbead size is crucial in the experiment, ensuring maximized sensor performance and facilitating smooth preparation processes.

We also investigated the relationship between the electrospinning time and the sensor sensitivity, because the thickness of the nanofiber membrane is directly determined by the electrospinning time, and the membrane thickness is usually an important factor affecting the membrane performance. Relative changes in resistance depending on pressure are shown in Fig. 3.

When the electrospinning time of nanofibers is 5 min, the resistance value of the corresponding sensor changes little in the whole pressure range. Possible reasons are as follows. The number of nanofibers prepared by a short-time electrospinning process is too small to fully cover the microbeads. Compared to PVDF nanofibers, the microbeads exhibit better stress resistance due to the rigidity of PMMA. Therefore, through the separation of the microbeads, the conductive layer in the upper electrode is difficult to contact with the lower electrode and the sensor works entirely on the elasticity of the bead.

According to our previous study, when the electrospinning time is increased to 20 min, the thickness of the film is slightly larger than the diameter of the microbead. Therefore, most of the microbeads are wrapped by nanofibers, and no microbeads will protrude completely from the surface of the nanofiber membrane. As can be seen from the Fig. 3a, in the initial stage of the pressure-response curve, the curve rises very quickly. This is because when the sensor is subjected to external pressure, microbeads that protrude slightly from the surface can be easily pressed into the membrane. At this stage, the resilience to external pressure is primarily attributed to the nanofibers, resulting in a membrane surface that is readily susceptible to flattening, that is, the resistance change easily reaches saturation. With the increase of external pressure, the pressure-response curve exhibits a gradual attenuation. This phenomenon is attributed to two primary factors. Firstly, the presence of internal hard microbeads, which act as spacers, effectively hinders the rapid thinning of the membrane when subjected to external forces. These microbeads provide mechanical support, maintaining the membrane's structural integrity. Secondly, the existence of surface pores increases the contact area between the membrane and the electrode during the thinning process. This enlargement of the contact area enhances the interaction between the membrane and electrode, influencing the overall performance of the system. As can be seen from the Fig. S5 the pores in the 20-min sample are deeper than those in the 5-min sample. Therefore, conductive AgNWs sprayed onto the membrane surface are more likely to trap into the pores. Consequently, under a certain pressure load, the contact area between the electrodes and the conductive AgNWs within the pores increases due to the membrane thinning.

To assess the impact of an extended preparation time on the

membrane, we also prepared membranes with an electrospinning time of 60 min. The pressure-response curve analysis shows that the sensitivity of the 60-min sample is as high as  $1.12 \text{ kPa}^{-1}$ . This may be because thicker membranes have better resistance to external pressure. The linearity ( $R^2$ ) of the samples under a pressure range of 20–500 Pa was also evaluated for different sample preparation durations: 5 min ( $R^2 = 0.65$ ), 20 min ( $R^2 = 0.80$ ), and 60 min ( $R^2 = 0.83$ ). These results indicate that extending the preparation time improves the linearity, suggesting enhanced sample uniformity or structural stability with longer preparation durations. However, the linearity of the 60-min sample did not exhibit a significant improvement. This may be because the thickness of the nanofiber membrane is much larger than the diameter of the microbeads, and the microbeads still play the role of main spacers in this sample. Moreover, in the saturation region of the pressure-response curve (i.e., external pressure greater than 2 kPa), the resistance changes of the 60-min sample ( $\Delta R/R_0 = 0.5$ ) exhibited a limited improvement compared to that of the 20-min sample ( $\Delta R/R_0 = 0.3$ ). Despite the fabrication time being tripled, the resistance change did not show a corresponding threefold increase. Similar to the previous study, prolonging the electrospinning time of nanofibers does not linearly increase their thickness. This observation indicates that merely extending the electrospinning time does not indefinitely enhance the sensor's performance. On the contrary, it significantly elevates the production cost of the nanofiber membrane. In summary, choosing the appropriate electrospinning time for nanofibers is crucial for fabricating pressure sensors in this study.

The hysteresis performance of a pressure sensor is a crucial aspect for its reliability and accuracy in various applications. We performed a hysteresis test on the sensor corresponding to the nanofiber obtained by electrospinning for 60 min. As shown in Fig. 3b, the hysteresis loop shows a negligible deviation between the ascending and descending pressure cycles. The hysteresis of the curve is calculated using the following formula, and the final result is found to be 0.63 %.

$$\text{hysteresis} = \frac{\int_{\text{unloading}} (R_0 - R)/R_0 dp - \int_{\text{loading}} (R_0 - R)/R_0 dp}{[(R_0 - R)/R_0]_{\text{max}} P_{\text{max}}}$$

This indicates that the sensor output demonstrates excellent repeatability and stability. Hysteresis performance results show that the nanofiber sensor has excellent properties, highlighting the sensor's capability to precisely capture dynamic pressure changes with minimal hysteresis. This excellent performance is attributed to the precise structural design and material properties of the sensing elements.

We also evaluated the effect of high microbead content on the performance of pressure sensors (Fig. 3c). For this purpose, we prepared a series of nanofiber membranes by incorporating high concentrations of microbeads into the PVDF electrospinning solution. The mass ratio of PVDF to microbeads in these membranes was 1:0.4. Afterwards, sensors were prepared based on the nanofiber membranes obtained at different electrospinning times.

We found that the performance of the pressure sensor corresponding to the nanofibers obtained by electrospinning for 5 min was similar to that of the sample with low bead content (mass ratio of PVDF to

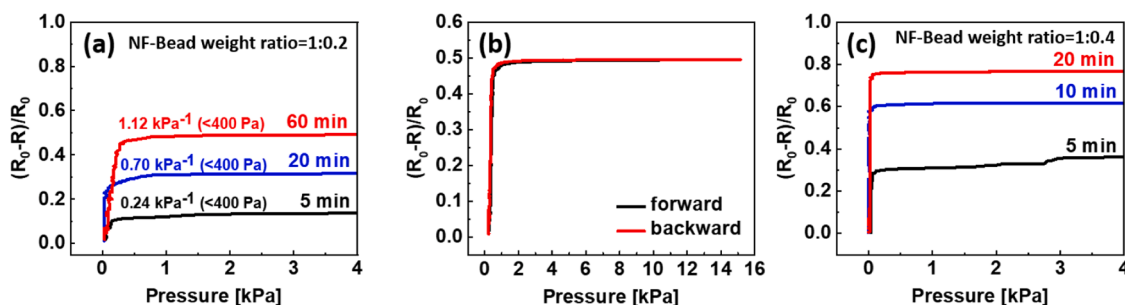


Fig. 3. Impact of (a) preparation time, (b) hysteresis, and (c) high microbead content on the performance of the piezoresistive pressure sensor.

microbeads is 1:0.2). The reason for this observation could be attributed to the fact that after a short electrospinning duration, the thickness of the formed nanofiber membrane is smaller than the diameter of the microbeads. Consequently, the microbeads protrude from the surface of the nanofiber membrane. Therefore, the microbeads become the main separators, and the external pressure is mainly applied on the microbeads. This explains why the 5-min sample maintains a certain degree of linearity, while an increase in bead concentration at this point has little effect on sensor performance.

However, for the samples electrospun for 10 and 20 min, the pressure-response curves saturated at low pressures, rendering these pressure sensors almost unusable in practical applications. This may be because increasing the bead concentration can effectively increase the thickness of the nanofiber membrane. As the electrospinning time increases, the overall thickness of the membrane increases, and the microbeads are completely buried inside the nanofibers, leaving almost no protrusions on the surface of the nanofiber membrane. This results in complete contact between the upper and lower electrodes of the sensor under low pressure, leading to saturation in pressure response.

In addition, although the pressure-response curves of the three samples all reach saturation at low pressures, the total resistance changes are different within the measurable pressure range. Therefore, the surface morphology of the three nanofiber membranes was analyzed by SEM, and the results are shown in Fig. S5. Since the 5-min sample is very thin, we can easily distinguish the nanofibers from the substrate. Except for a few microbeads protruding from the surface, the nanofiber membrane is relatively flat, and the coverage of silver nanowires is high. This confirms our previous speculation. However, as the electrospinning time increases, the holes on the surface of the nanofiber membrane increase, and the coverage of silver nanowires between nanofibers significantly decreases. When there is no external pressure, the contact area between the upper and lower electrodes is small, resulting in a large initial resistance of the sensor. As the external pressure increases, the film thickness decreases, causing the silver nanowires in the holes to be exposed and contact the lower electrode, reducing the contact resistance between the upper and lower electrodes.

In summary, the sensing mechanism of the piezoresistive pressure sensor is based on the pressure-induced change in resistance, which occurs due to the interplay of structural features within the membrane. When external pressure is applied, internal hard microbeads act as spacers, limiting excessive membrane thinning and maintaining structural stability. Simultaneously, surface pores on the membrane increase the contact area with the electrode as the membrane thins, enhancing the interaction between the two. These combined effects result in a gradual resistance decrease with increasing pressure, enabling accurate pressure sensing. Several nanofiber membranes were prepared according to different electrospinning conditions. By comparing and analyzing the sensitivity performance of the pressure sensors, we found that the preparation conditions of the nanofibers are the main factors affecting

the final pressure sensors. Based on this result, we designed the nanofiber electrode by optimizing the preparation conditions, which significantly improved the performance of the sensor.

### 3.4. Stability

The dynamic response curves of the pressure sensor prepared in the experiment to different pressures are shown in Fig. 4a. We applied different pressures (200 Pa, 400 Pa, 800 Pa, 1.6 kPa, 5 kPa) to the sensor and repeated the pressing 5 times for each pressure. The sensor exhibits a stable and reliable response to the same pressure, and the response is consistent with the previous pressure-response curve. In addition, sensors based on nanofibers containing microbeads have fast response and recovery times. By pressing the pressure sensor with a pressure of 400 Pa and holding it for 1 s, and then removing the pressure, the response/recovery time of the piezoresistive pressure sensor can be measured, which are 210 ms and 140 ms, respectively (Fig. 4b). This shows that the sensor can quickly respond to external pressure and meet the requirements for rapid detection.

As shown in Fig. 5, we studied the stability and durability of the sensor by performing 1000 loading-unloading cycles under a pressure of 400 Pa. The procedural sequence encompasses four discrete steps: pressure loading, sustained compression for 1 s, pressure unloading, and a subsequent 1 s interval of inactivity. The speed of pressure loading and unloading was set to  $10 \text{ mm} \cdot \text{min}^{-1}$ . After 1000 cycles of loading and unloading process, the response value of the sensor has hardly decreased. At approximately the 400th cycle, we selected 13 response and recovery cycles to evaluate the stability. As shown in the inset, the changes in each cycle are consistent, which illustrates the good repeatability of the sensor.

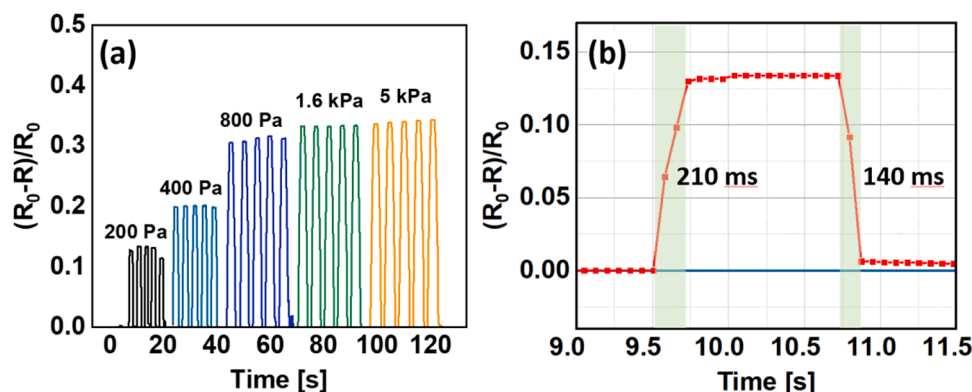


Fig. 4. (a) Dynamic response curves of the pressure sensor, (b) response/recovery time of the pressure sensor.

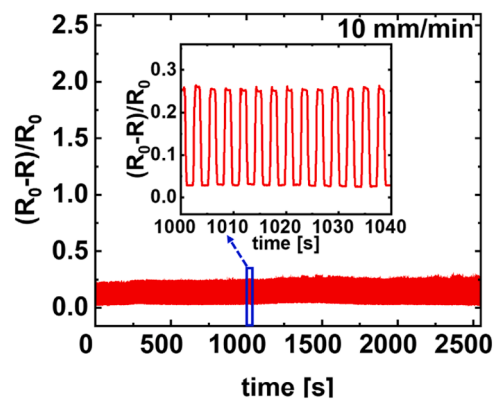


Fig. 5. Stability of the sensor through 1000 loading-unloading cycles under a pressure of 400 Pa. Inset shows an enlarged view around the 400th cycle.

### 3.5. Application of pressure sensors in human body pulse measurement

Since the nanofibrous membrane is a flexible material, and the AgNWs used as the conductive electrode material also have excellent flexibility, so the proposed pressure sensor can be used for pressure detection on curved surfaces. In a real-time pressure detection demonstration, a nanofiber-based pressure sensor was placed on the surface of a measuring cylinder, then its surface was tapped with a finger and the resistance change was monitored. Fig. 6 shows the dynamic resistance changes of the flexible pressure sensor when detecting random finger touches on the cylinder surface. The results indicate that our pressure sensor is capable of sensing and distinguishing various pressure levels even when operating on a curved surface. This not only demonstrates the sensor's exceptional flexibility but also confirms that the ultra-thin sensing structure remains undamaged during bending. Moreover, it's noteworthy that each touch can be clearly differentiated, with the resistance value dropping sharply upon finger pressure and swiftly returning to its initial value upon release. This illustrates that the sensor maintains high accuracy and sensitivity even when functioning on a curved surface.

Bending behavior generally induces compression or stretching of the overall structure. However, the device in this study primarily relies on resistance changes in the conductive thin film on the nanofiber surface to detect external pressure. Previously, we constructed a similar sandwich-structured device comprising top and bottom carrier films and a nanofiber membrane [46]. After subjecting the device to 250 bending cycles, we observed no significant degradation in capacitance values across the nanofiber membrane, indicating its ability to recover its original morphology after stress removal. In this study, the nanofibers are thinner, further enhancing the mechanical stability of the structure under bending. This ensures that the thin sensing structure remains undamaged, maintaining its exceptional flexibility and reliable performance during repeated bending cycles.

Based on the experimental results and analysis provided, we have developed a flexible piezoresistive pressure sensor with exceptional sensitivity. This sensor not only demonstrates the ability to detect low pressure effectively but also boasts a fast response time and outstanding stability. These characteristics make it well-suited for high-precision dynamic pressure sensing applications. To illustrate its practicality, we conducted tests utilizing human-body pulse waveforms.

Pulse waveform is an important feedback of human health information. By analyzing the pulse waveform data, information such as heart rate and cardiovascular status can be obtained [52]. It is of great medical significance in helping to diagnose hypertension, arteriosclerosis, and other cardiovascular diseases and is also an important application of electronic skin devices. Usually, the pulse monitoring by an electronic skin is achieved through pressure or strain sensors. Specifically, the pressure or strain sensor is attached or fixed at a position where the pulse can be sensed. When the artery pulsates periodically,

the pressure sensor undergoes compression or relaxation, detecting the signal which is then plotted into a waveform for subsequent analysis.

Fig. 7 illustrates the continuous monitoring of carotid artery and wrist artery pulse signals from the same volunteer over a span of 8.0 s. Each pulse signal exhibited a consistent pattern akin to that of a healthy 30-year-old male. Our proposed pressure sensor, with a thickness of less than 80  $\mu\text{m}$ , can be securely affixed using only tape for health monitoring, providing significant convenience in practical applications. Notably, the sensor demonstrated stable and clear recording of pulse waveforms in both tests. Additionally, the signal amplitude of the carotid artery notably exceeded that of the wrist artery pulse signal, which is consistent with real-world observations. Examining the enlarged view, each cycle of the arterial waveform comprises three characteristic peaks, and the correlation between these peaks can provide insights into the cardiovascular function condition. This is mainly due to the sensor's high sensitivity, high repeatability and fast response time. The above results show that highly sensitive and flexible pressure sensors based on nanofiber membranes have broad application prospects in the field of high-precision dynamic pressure sensing, especially in human-computer interaction and health monitoring.

## 4. Conclusions

In this paper, we proposed a strategy for designing a novel flexible piezoresistive pressure sensor based on a nanofiber-microbead composite membrane. The microstructure is realized by nanofibers containing micron-sized beads, and the regulation of sensitivity and linearity is achieved by controlling the preparation conditions of the nanofiber composites. By studying the sensing properties of the nanofiber based piezoresistive flexible pressure sensors, we noticed that the integration of microbeads is beneficial for improving the performance of pressure sensors based on nanofibers. Nevertheless, the presence of microbeads with high content can induce sensor saturation within the low-pressure region. In addition, choosing an appropriate electrospinning time for nanofiber is also crucial for fabricating pressure sensors. Finally, a flexible pressure sensor has been developed that exhibits high sensitivity of  $1.12 \text{ kPa}^{-1}$ , low hysteresis deviation, fast response and recovery times of 210 ms and 140 ms, respectively, and good stability over 1000 repetitive pressings. The sensor has been effectively demonstrated to operate on curved surfaces and can be attached to human skin, allowing real-time monitoring of wrist pulses and carotid pulses due to its outstanding sensing performance. It is believed that the proposed flexible pressure sensor with simple fabrication, low cost, high sensitivity and good stability can have broad application prospects in the fields of bionic electronic skin, wearable devices and future rehabilitation monitoring.

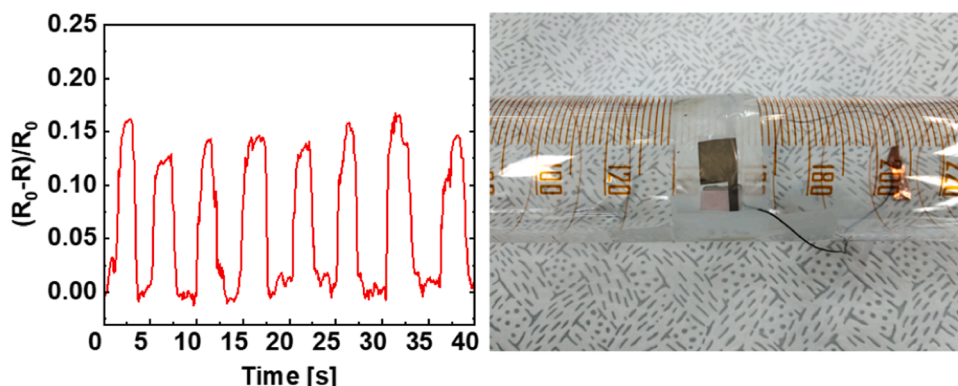


Fig. 6. Dynamic resistance changes of the flexible pressure sensor when detecting random finger touches on a cylinder surface.

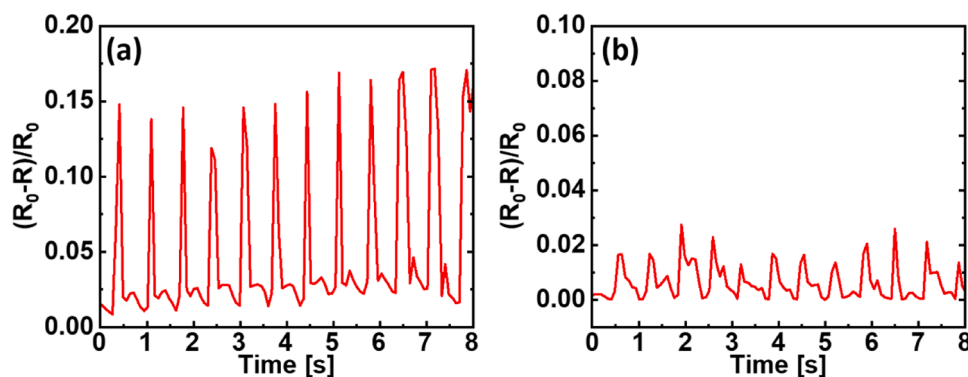


Fig. 7. Continuous monitoring of (a) carotid artery and (b) wrist artery pulse signals from the same volunteer over an 8.0 s duration.

### CRediT authorship contribution statement

**Sang-Hee Ko Park:** Writing – review & editing, Resources. **Yan Pan:** Writing – review & editing, Investigation. **Taiyu Jin:** Writing – original draft, Visualization, Methodology, Data curation, Conceptualization. **Da-Wei Fang:** Writing – review & editing, Funding acquisition, Conceptualization.

### Declaration of Competing Interest

The authors declare that they have no known competing financial interests or personal relationships that could have appeared to influence the work reported in this paper.

### Acknowledgements

This work is financially supported by NSFC (22173039), Liaoning Revitalization Talents Program (XLYC2202040), General Program of Liaoning Provincial Department of Education (LJKFZ20220178), Key Technologies R & D Program of Liaoning Provincial Department of Education (LJKZZ20220018), and China Scholarship Council (CSC) Grant (202306800007).

### Appendix A. Supporting information

Supplementary data associated with this article can be found in the online version at [doi:10.1016/j.jallcom.2025.178609](https://doi.org/10.1016/j.jallcom.2025.178609).

### Data availability

Data will be made available on request.

### References

- Y. Zang, F. Zhang, C. Di, D. Zhu, Advances of flexible pressure sensors toward artificial intelligence and health care applications, *Mater. Horiz.* 2 (2015) 140–156, <https://doi.org/10.1039/c4mh00147h>.
- Y.-G. Park, G.-Y. Lee, J. Jang, S.M. Yun, E. Kim, J.-U. Park, Liquid metal-based soft electronics for wearable healthcare, *Adv. Healthc. Mater.* 10 (2021) 2002280, <https://doi.org/10.1002/adhm.202002280>.
- J. Luo, S. Gao, H. Luo, L. Wang, X. Huang, Z. Guo, X. Lai, L. Lin, R.K.Y. Li, J. Gao, Superhydrophobic and breathable smart MXene-based textile for multifunctional wearable sensing electronics, *Chem. Eng. J.* 406 (2021) 126898, <https://doi.org/10.1016/j.cej.2020.126898>.
- Y. Li, X. Wei, Z. Liu, H. Kang, W. Han, Flexible and breathable piezoresistive sensors based on reduced graphene oxide/silk fiber/carbon cloth composites for health monitoring, *ACS Appl. Nano Mater.* 7 (2024) 8813–8822, <https://doi.org/10.1021/acsnm.4c00286>.
- R. Yang, W. Zhang, N. Tiwari, H. Yan, T. Li, H. Cheng, Multimodal sensors with decoupled sensing mechanisms, *Adv. Sci.* 9 (2022) 2202470, <https://doi.org/10.1002/advs.202202470>.
- Q. Huang, Y. Jiang, Z. Duan, Y. Wu, Z. Yuan, M. Zhang, H. Tai, Ion gradient induced self-powered flexible pressure sensor, *Chem. Eng. J.* 490 (2024) 151660, <https://doi.org/10.1016/j.cej.2024.151660>.
- X. Feng, Y. Ran, X. Li, H. Xu, Q. Huang, Z. Duan, Z. Yuan, Y. Jiang, H. Tai, Amorphous carbon derived from daily carbon ink for wide detection range, low-cost, eco-friendly and flexible pressure sensor, *Mater. Chem. Phys.* 321 (2024) 129489, <https://doi.org/10.1016/j.matchemphys.2024.129489>.
- T. Li, Z. Duan, Q. Huang, H. Yang, Z. Yuan, Y. Jiang, H. Tai, *Sens. Actuator A Phys.* 376 (2024) 115629, <https://doi.org/10.1016/j.sna.2024.115629>.
- Z. Huang, Z. Duan, Q. Huang, Z. Yuan, Y. Jiang, H. Tai, *J. Mater. Chem. C* 12 (2024) 18320–18326, <https://doi.org/10.1039/d4tc03434a>.
- Q. Huang, Y. Jiang, Z. Duan, Z. Yuan, Y. Wu, J. Peng, Y. Xu, H. Li, H. He, H. Tai, A finger motion monitoring glove for hand rehabilitation training and assessment based on gesture recognition, *IEEE Sens. J.* 23 (12) (2023) 13789–13796, <https://doi.org/10.1109/JSEN.2023.3264620>.
- Q. Yu, C. Su, S. Bi, Y. Huang, J. Li, H. Shao, J. Jiang, N. Chen,  $\text{Ti}_3\text{C}_2\text{T}_x$ @nonwoven fabric composite: promising mxene-coated fabric for wearable piezoresistive pressure sensors, *ACS Appl. Mater. Interfaces* 14 (7) (2022) 9632–9643, <https://doi.org/10.1021/acsnm.2c00980>.
- X. Lin, H. Xue, F. Li, H. Mei, H. Zhao, T. Zhang, All-nanofibrous ionic capacitive pressure sensor for wearable applications, *ACS Appl. Mater. Interfaces* 14 (27) (2022) 31385–31395, <https://doi.org/10.1021/acsnm.2c01806>.
- C. Wang, D. Gong, P. Feng, Y. Cheng, X. Cheng, Y. Jiang, D. Zhang, J. Cai, Ultra-sensitive and wide sensing-range flexible pressure sensors based on the carbon nanotube film/stress-induced square frustum structure, *ACS Appl. Mater. Interfaces* 15 (6) (2023) 8546–8554, <https://doi.org/10.1021/acsnm.2c22727>.
- T. Jin, S.-H.K. Park, D.-W. Fang, Highly-stable flexible pressure sensor using piezoelectric polymer film on metal oxide TFT, *RSC Adv.* 12 (2022) 21014–21021, <https://doi.org/10.1039/d2ra02613a>.
- S. Lee, J.-W. Park, Fingerprint-inspired triboelectric nanogenerator with a geometrically asymmetric electrode design for a self-powered dynamic pressure sensor, *Nano Energy* 101 (2022) 107546, <https://doi.org/10.1016/j.nanoen.2022.107546>.
- L. Shi, Z. Li, M. Chen, Y. Qin, Y. Jiang, L. Wu, Quantum effect-based flexible and transparent pressure sensors with ultrahigh sensitivity and sensing density, *Nat. Commun.* 11 (2020) 3529, <https://doi.org/10.1038/s41467-020-17298-y>.
- C.-Y. Tang, X. Zhao, J. Jia, S. Wang, X.-J. Zha, B. Yin, K. Ke, R.-Y. Bao, Z.-Y. Liu, Y. Wang, K. Zhang, M.-B. Yang, W. Yang, Low-entropy structured wearable film sensor with piezoresistive-piezoelectric hybrid effect for 3D mechanical signal screening, *Nano Energy* 90 (2021) 106603, <https://doi.org/10.1016/j.nanoen.2021.106603>.
- Z. Ji, L. Zhang, J. Zhou, J. Jiang, P. Cao, Highly sensitive, wide-sensing-range rGO/NiMoO@CMF pressure sensor based on biomimetic mimosa flowers for health monitoring and human-computer interaction, *ACS Appl. Nano Mater.* 7 (8) (2024) 8949–8957, <https://doi.org/10.1021/acsnm.4c00446>.
- X. Ding, Y. Cai, G. Lu, J. Hu, J. Zhao, L. Zheng, Z. Weng, H. Cheng, J. Lin, L. Wu, Stretchable superhydrophobic elastomers with on-demand tunable wettability for droplet manipulation and multi-stage reaction, *J. Mater. Chem. C* 11 (2023) 10069–10078, <https://doi.org/10.1039/d3tc01666h>.
- C. Zhang, H.M. Chen, X.H. Ding, F. Lorestani, C.L. Huang, B.W. Zhang, B. Zheng, J. Wang, H.Y. Cheng, Y. Xu, Human motion-driven self-powered stretchable sensing platform based on laser-induced graphene foams, *Appl. Phys. Rev.* 9 (2022) 011413, <https://doi.org/10.1063/5.0077667>.
- R.X. Yang, A. Dutta, B.W. Li, N. Tiwari, W.Q. Zhang, Z.Y. Niu, Y.Y. Gao, D. Erdelyi, X. Xin, T.J. Li, H.Y. Cheng, Iontronic pressure sensor with high sensitivity over ultra-broad linear range enabled by laser-induced gradient micro-pyramids, *Nat. Commun.* 14 (2023) 2907, <https://doi.org/10.1038/s41467-023-38274-2>.
- M.H. Cao, M. Leng, W.L. Pan, Y.L. Wang, S.Z. Tan, Y.P. Jiao, S.G. Yu, S.Q. Fan, T. Xu, T. Liu, L. Li, J. Su, 3D wearable piezoresistive sensor with waterproof and antibacterial activity for multimodal smart sensing, *Nano Energy* 112 (2023) 108492, <https://doi.org/10.1016/j.nanoen.2023.108492>.
- G. Yang, M.Z. Tian, P. Huang, Y.F. Fu, Y.Q. Li, Y.Q. Fu, X.Q. Wang, Y. Li, N. Hu, S. Y. Fu, Flexible pressure sensor with a tunable pressure-detecting range for various human motions, *Carbon* 173 (2021) 736–743, <https://doi.org/10.1016/j.carbon.2020.11.066>.
- R. Yu, T.C. Xia, B. Wu, J. Yuan, L.J. Ma, G.J. Cheng, F. Liu, Highly sensitive flexible piezoresistive sensor with 3D conductive network, *ACS Appl. Mater. Interfaces* 12 (2020) 35291–35299, <https://doi.org/10.1021/acsnm.0c09552>.

- [25] M.Q. Jian, K.L. Xia, Q. Wang, Z. Yin, H.M. Wang, C.Y. Wang, H.H. Xie, M.C. Zhang, Y.Y. Zhang, Flexible and highly sensitive pressure sensors based on bionic hierarchical structures, *Adv. Funct. Mater.* 27 (2017) 1606066, <https://doi.org/10.1002/adfm.201606066>.
- [26] C.L. Choong, M.B. Shim, B.S. Lee, S. Jeon, D.S. Ko, T.H. Kang, J. Bae, S.H. Lee, K. E. Byun, J. Im, Y.J. Jeong, C.E. Park, J.J. Park, U.I. Chung, Highly stretchable resistive pressure sensors using a conductive elastomeric composite on a micropyramid array, *Adv. Mater.* 26 (2014) 3451–3458, <https://doi.org/10.1002/adma.201305182>.
- [27] C. Pang, G.Y. Lee, T.I. Kim, S.M. Kim, H.N. Kim, S.H. Ahn, K.Y. Suh, A flexible and highly sensitive strain-gauge sensor using reversible interlocking of nanofibres, *Nat. Mater.* 11 (2012) 795–801, <https://doi.org/10.1038/nmat3380>.
- [28] J.F. Yan, Y.A. Ma, G. Jia, S.R. Zhao, Y. Yue, F. Cheng, C.K. Zhang, M.L. Cao, Y. C. Xiong, P.Z. Shen, Y.H. Gao, Bionic MXene based hybrid film design for an ultrasensitive piezoresistive pressure sensor, *Chem. Eng. J.* 431 (2022) 133458, <https://doi.org/10.1016/j.cej.2021.133458>.
- [29] Y.W. Lu, Y. He, J.T. Qiao, X. Niu, X.J. Li, H. Liu, L. Liu, Highly sensitive interlocked piezoresistive sensors based on ultrathin ordered nanocone array films and their sensitivity simulation, *ACS Appl. Mater. Interfaces* 12 (2020) 55169, <https://doi.org/10.1021/acsaami.0c16456>.
- [30] B.D. Chen, L. Zhang, H.Q. Li, X.J. Lai, X.R. Zeng, Skin-inspired flexible and high-performance MXene@polydimethylsiloxane piezoresistive pressure sensor for human motion detection, *J. Colloid Interface Sci.* 617 (2022) 478–488, <https://doi.org/10.1016/j.jcis.2022.03.013>.
- [31] W.D. Li, J.H. Pu, X. Zhao, J. Jia, K. Ke, R.Y. Bao, Z.Y. Liu, M.B. Yang, W. Yang, Scalable fabrication of flexible piezoresistive pressure sensors based on occluded microstructures for subtle pressure and force waveform detection, *J. Mater. Chem. C* 8 (2020) 16774, <https://doi.org/10.1039/d0tc03961f>.
- [32] C. Yu, J. Xu, L. Yang, M. Ye, Y. Ye, T. Li, Y. Zhang, Z. Zhang, H. Xu, H. Tan, G. Zhang, H. Zhang, Self-driving flexible piezoresistive sensors integrated with enhanced energy harvesting sensor of ZnO/Ti<sub>3</sub>C<sub>2</sub>T<sub>x</sub> nanocomposite based on 3D structure, *J. Alloy. Compd.* 956 (2023) 170358, <https://doi.org/10.1016/j.jallcom.2023.170358>.
- [33] W. Song, R. Xiao, Covalently interconnected thermoplastic polymeric nanofiber/carbon nanotube composite nanofibrous aerogels for piezoresistive sensors, *ACS Appl. Nano Mater.* 7 (2024) 7510–7519, <https://doi.org/10.1021/acsnan.4c00080>.
- [34] X. Guo, W. Hong, B. Hu, T. Zhang, C. Jin, X. Yao, H. Li, Z. Yan, Z. Jiao, M. Wang, B. Ye, S. Wei, Y. Xia, Q. Hong, Y. Xu, Y. Zhao, Human touch sensation-inspired, ultrawide-sensing-range, and high-robustness flexible piezoresistive sensor based on CB/MXene/SR/fiber nanocomposites for wearable electronics, *Compos. Struct.* 321 (2023) 117329, <https://doi.org/10.1016/j.compstruct.2023.117329>.
- [35] Y. Zhu, M.C. Hartel, N. Yu, P.R. Garrido, S. Kim, J. Lee, P. Bandaru, S. Guan, H. Lin, S. Emaminejad, N.R. deBarros, S. Ahadian, H.-J. Kim, W. Sun, V. Jucaud, M. R. Dokmeci, P.S. Weiss, R. Yan, A. Khademhosseini, Epidermis-inspired wearable piezoresistive pressure sensors using reduced graphene oxide self-wrapped copper nanowire networks, *Small Methods* 6 (2022) 2100900, <https://doi.org/10.1002/smt.202100900>.
- [36] D.M. dos Santos, D.S. Correa, E.S. Medeiros, J.E. Oliveira, L.H.C. Mattoso, Advances in functional polymer nanofibers: from spinning fabrication techniques to recent biomedical applications, *ACS Appl. Mater. Interfaces* 12 (2020) 45673–45701, <https://doi.org/10.1021/acsaami.0c12410>.
- [37] F.J. Jiang, Y. Nie, L. Yin, Y. Feng, Q.C. Yu, C.Y. Zhong, Core-shell-structured nanofibrous membrane as advanced separator for lithium-ion batteries, *J. Membr. Sci.* 510 (2016) 1–9, <https://doi.org/10.1016/j.memsci.2016.02.067>.
- [38] J.W. Xu, C. Liu, P.C. Hsu, K. Liu, R.F. Zhang, Y.Y. Liu, Y. Cui, Roll-to-roll transfer of electrospun nanofiber film for high-efficiency transparent air filter, *Nano Lett.* 16 (2) (2019) 1270–1275, <https://doi.org/10.1021/acs.nanolett.5b04596>.
- [39] W. Liang, Y. Xu, X. Li, X.X. Wang, H.D. Zhang, M. Yu, S. Ramakrishna, Y.Z. Long, Transparent polyurethane nanofiber air filter for high-efficiency PM2.5 capture, *Nanoscale Res. Lett.* 14 (2019) 361, <https://doi.org/10.1186/s11671-019-3199-0>.
- [40] M.F. Lin, J.Q. Xiong, J.X. Wang, K. Parida, P.S. Lee, Core-shell nanofiber mats for tactile pressure sensor and nanogenerator applications, *Nano Energy* 44 (2018) 248–255, <https://doi.org/10.1016/j.nanoen.2017.12.004>.
- [41] W. Yang, N.W. Li, S.Y. Zhao, Z.Q. Yuan, J.N. Wang, X.Y. Du, B. Wang, R. Cao, X. Y. Li, W.H. Xu, Z.L. Wang, C.J. Li, A breathable and screen-printed pressure sensor based on nanofiber membranes for electronic skins, *Adv. Mater. Technol.* 3 (2) (2018) 1700241, <https://doi.org/10.1002/admt.201700241>.
- [42] W.J. Liu, N.S. Liu, Y. Yue, J.Y. Rao, F. Cheng, J. Su, Z.T. Liu, Y.H. Gao, Piezoresistive pressure sensor based on synergistical innerconnect polyvinyl alcohol nanowires/wrinkled graphene film, *Small* 14 (15) (2018) 1704149, <https://doi.org/10.1002/sml.201704149>.
- [43] X.H. Hu, Y.G. Jiang, Z.Q. Ma, Q.P. He, Y.P. He, T.F. Zhou, D.Y. Zhang, Highly sensitive P(VDF-TrFE)/BTO nanofiber-based pressure sensor with dense stress concentration microstructures, *ACS Appl. Polym. Mater.* 2 (11) (2020) 4399–4404, <https://doi.org/10.1021/acsaapm.0c00411>.
- [44] M. Ren, J. Li, L. Lv, M. Zhang, X. Yang, Q. Zhou, D. Wang, R. Dhakal, Z. Yao, Y. Li, N.Y. Kim, A wearable and high-performance capacitive pressure sensor based on a biocompatible PVP nanofiber membrane via electrospinning and UV treatment, *J. Mater. Chem. C* 10 (2022) 10491–10499, <https://doi.org/10.1039/d2tc00955b>.
- [45] Y. Kim, S. Jang, B.J. Kang, J.H. Oh, Fabrication of highly sensitive capacitive pressure sensors with electrospun polymer nanofibers, *Appl. Phys. Lett.* 111 (2017) 073502, <https://doi.org/10.1063/1.4998465>.
- [46] T. Jin, Y. Pan, G.-J. Jeon, H.-J. Yeom, S. Zhang, K.-W. Paik, S.-H.K. Park, Ultrathin nanofibrous membranes containing insulating microbeads for highly sensitive flexible pressure sensors, *ACS Appl. Mater. Interfaces* 12 (11) (2020) 13348–13359, <https://doi.org/10.1021/acsaami.0c00448>.
- [47] L.J. Pan, A. Chortos, G.H. Yu, Y.Q. Wang, S. Isaacson, R. Allen, Y. Shi, R. Dauskardt, Z.N. Bao, An ultra-sensitive resistive pressure sensor based on hollow-sphere microstructure induced elasticity in conducting polymer film, *Nat. Commun.* 5 (2014) 3002, <https://doi.org/10.1038/ncomms4002>.
- [48] C.Y. Li, H. Gu, Z.Y. Ji, L.M. Zhang, R.X. Xu, J.Y. Gao, Y. Jiang, Hierarchically structured MXene nanosheets on carbon sponges with a synergistic effect of electrostatic adsorption and capillary action for highly sensitive pressure sensors, *ACS Appl. Nano Mater.* 6 (14) (2023) 13482, <https://doi.org/10.1021/acsaam.3c02126>.
- [49] T.Y. Shao, J.N. Wu, Y.H. Zhang, Y.R. Cheng, Z.Q. Zuo, H.K. Lv, M.L. Ying, C. P. Wong, Z. Li, Highly sensitive conformal pressure sensing coatings based on thermally expandable microspheres, *Adv. Mater. Technol.* 5 (2020) 2000032, <https://doi.org/10.1002/admt.202000032>.
- [50] G.F. He, F.G. Ning, X. Liu, Y.X. Meng, Z.W. Lei, X.D. Ma, M.W. Tian, X.Q. Liu, X. S. Zhang, X.J. Zhang, L.J. Qu, High-performance and long-term stability of MXene/PEDOT:PSS-decorated cotton yarn for wearable electronics applications, *Adv. Fiber Mater.* 6 (2024) 367–386, <https://doi.org/10.1007/s42765-023-00348-7>.
- [51] C.B. Huang, S. Witomska, A. Aliprandi, M.A. Stoeckel, M. Bonini, A. Ciesielski, P. Samori, Molecule-graphene hybrid materials with tunable mechanoresponse: highly sensitive pressure sensors for health monitoring, *Adv. Mater.* 31 (1) (2019) 1804600, <https://doi.org/10.1002/adma.201804600>.
- [52] Y.J. Wang, Y. Wang, M.T. Xu, F.Y. Dai, Z. Li, Flat silk cocoon pressure sensor based on a sea urchin-like microstructure for intelligent sensing, *ACS Sustain. Chem. Eng.* 10 (51) (2022) 17252–17260, <https://doi.org/10.1021/acssuschemeng.2c05540>.